



# Thermodynamic analysis of novel mixtures including siloxanes and cyclic hydrocarbons for high-temperature heat pumps

Echezona Obika<sup>a,b,\*</sup>, Florian Heberle<sup>a</sup>, Dieter Brüggemann<sup>a</sup>

<sup>a</sup> Chair of Engineering Thermodynamics and Transport Processes (LTTT), Center of Energy Technology (ZET), University of Bayreuth, Universitätsstraße 30, 95447, Bayreuth, Germany

<sup>b</sup> Department of Mechanical Engineering, Nnamdi Azikiwe University, Awka, P.M.B. 5025, Awka, Anambra State, Nigeria

## ARTICLE INFO

Handling editor: Yunho Hwang

### Keywords:

Vapor compression  
Heat pump  
Hexamethyldisiloxane  
Cyclopropane  
Cyclohexane  
Temperature glide  
Exergy  
COP  
Zeotropic mixtures

## ABSTRACT

This paper presents the investigation of zeotropic binary fluid mixtures containing cyclohexane (critical temperature above 200 °C) as the base fluid with R600, R600a, R601, R601a, R1336mzz(Z), R1234ze(Z), R1233zd(E) and cyclopropane (critical temperatures between 100 °C and 200 °C). For pure components and their mixtures, the performance of the vapor compression system with an internal heat exchanger was analysed at 50 °C and 80 °C heat source and sink inlet, respectively. Variation of the heat source temperature difference and the internal heat exchanger pinch point temperature difference at supply temperatures (140–170 °C) were also investigated. A pinch point temperature difference of 5 K was maintained for the evaporator and condenser. An increase of 6.59 % in COP was obtained with the zeotropic mixture of cyclohexane/cyclopropane compared to that of pure cyclopropane. The design point analysis showed that increasing the heat source temperature difference and internal heat exchanger pinch point temperature difference reduces the COP. The adopted mixture criteria increased the performance between 3.23 % and 3.91 % with respect to standard working fluids like R1233zd(E) and R601, for a 170 °C supply temperature. With this promising thermodynamic analysis in a subcritical operation, the cyclohexane/cyclopropane mixture has prospect of full integration heat pump design.

## 1. Introduction

Thermal energy is one form of energy with increasing need cutting across virtually all sectors of the economy. Its application include; space heating and hot water supply in buildings [1–5], drying, pasteurization as well as distillation [6]. It has been estimated that about two thirds of the energy consumption in the EU is in the form of heat and electricity [7]. The use of heat pumps is a very efficient means of providing this much needed heat. Its major advantage stems from its ability to utilize heat from various heat sources, which include waste heat from industries [3,7–10] and geothermal resources [11,12].

Various heat pump configurations have been studied in literature. They include a simple vapor compression system [13,14], vapor compression with internal heat exchanger [15], turbo compressor and thermal vapor recompression [16], cascaded systems [17,18], double source heat pumps [19] and recuperative air water heat pumps (RAWP) [20]. While system configuration plays an important role in performance [21], working fluid selection is also a key factor [22]. Recent

studies focus on improving the performance of heat pumps while avoiding negative environmental impacts associated with the use of certain working fluids. A fundamental step towards a proper heat pump design is the selection of the right working fluid suitable for the intended application. For high temperature applications, the critical temperature and pressure of the working fluids must be put into consideration. For low temperature applications, fluids with low boiling point and critical temperatures like R290 and CO<sub>2</sub>, have been studied by a number of researchers [8,20,23–26].

Due to environmental factors, natural working fluids like hydrocarbons have taken over the research space as possible replacement for synthetic working fluids like fluorinated hydrocarbons with known environmental impacts in recent times [27]. Among the hydrocarbons investigated for supply temperatures slightly above 100 °C are R600 [8, 21,27,28], R601 [20], R601a [20] and R600a [21,23]. Hydrocarbons generally have zero ozone layer depletion potential (ODP) and a negligible global warming potential (GWP). Nevertheless, due to their good compliance to environmental restrictions and performance, novel

\* Corresponding author. Chair of Engineering Thermodynamics and Transport Processes (LTTT), Center of Energy Technology (ZET), University of Bayreuth, Universitätsstraße 30, 95447, Bayreuth, Germany.

E-mail address: [Echezona.obika@uni-bayreuth.de](mailto:Echezona.obika@uni-bayreuth.de) (E. Obika).

<https://doi.org/10.1016/j.energy.2024.130858>

Received 17 July 2023; Received in revised form 26 February 2024; Accepted 27 February 2024

Available online 4 March 2024

0360-5442/© 2024 The Authors. Published by Elsevier Ltd. This is an open access article under the CC BY license (<http://creativecommons.org/licenses/by/4.0/>).

synthetic fluids such as R1336mzz(Z), R1234ze(Z) and R1233zd(E) are still relevant in heat pump research [21,29,30].

Research has shown that zeotropic mixtures improve the efficiency of thermodynamic cycles like heat pumps and organic Rankine cycles (ORC). The increase in performance associated with the use of zeotropic mixtures is linked to their temperature glide during phase change in the heat exchanger [23,31,32]. To attain this potential increase in performance, a mixture composition with suitable temperature glide matching must be identified along with other factors [23]. The findings of Sun et al. [33], for supply temperatures up to 72 °C on a single-stage compression air-source heat pump, showed that mixtures perform better only with good temperature glide matching. Fernández-Moreno et al. [28] showed that the blend of R1233zd(E) and R1336mzz(Z) was the most promising among several studied mixtures. For 130 °C supply temperature, the results of Deng et al. [34] gave a COP of 2.74 using NBY-1 (a mixture they developed). Xu et al. [35] investigated selected binary mixtures for 100 °C supply temperature increasing the COP of R245 by 9.51 % using its mixture named HG-1. Sun et al. [36] investigated different zeotropic fluid mixtures on a recuperative heat pump system to obtain a better temperature matching between the heat transfer fluid and working fluid, which the authors identified as the basis for improvement of the system performance. Thermodynamic analysis was conducted on eight heat pump configurations by Dai et al. [31] with the purpose of identifying good temperature glide matching. They concluded that the dual pressure configuration gives the best performance with good temperature glide, resulting in 3.37–9.34 % increase in COP. These researches show that irrespective of the plant configuration, a good temperature glide match must be identified for improved performance. Details regarding the investigated zeotropic mixtures, with configurations related to the vapor compression cycle, can be seen in Table 1. Additionally, relevant boundary conditions like supply and heat source temperatures also listed.

The current focus in heat pump research is on developing heat pumps capable of supplying temperatures higher than 130 °C. This is with the potential of serving as a viable replacement for industrial boilers [44]. However, hydrocarbons like hexane, cyclohexane and siloxanes, with high critical temperatures above 200 °C are scarcely investigated for high-temperature heat pump applications. In analogy to ORC applications, these high critical temperature fluids must be fully considered if the need for high temperature supply will be met. When utilized for low and medium temperature heat sources, these high critical temperature fluids are faced with the issue of very low evaporation pressure. This is a safety issue that must be considered when these fluids are used. This study addresses the gap in literature concerning the exploration of boundary conditions. Its objective is to enhance the efficiency of high-temperature heat pumps, specifically for delivery temperatures reaching up to 170 °C. This improvement is pursued through the utilization of either a pure working fluid or a combination of fluids with high and medium critical temperatures, falling within the range of 100 °C–200 °C. The novelty of this study lies in the investigation of high supply temperatures in the range of 140 °C and 170 °C. Also, cyclopropane, cyclopentane, hexamethyldisiloxane (MM) and their mixtures are yet to be investigated as working fluids in heat pumps. To meet the need for high temperature supplies, 11 working fluids have been pre-selected for this study. The vapor compression configuration with internal heat exchanger has been employed for better performance. A process simulation software is employed to simulate the entire thermodynamic cycle and the obtained results are correlated with findings in literature. Hence this study aims to answer the following research questions.

- Are ORC pure working fluids like siloxanes applicable to high temperature heat pumps?
- To what percentage can zeotropic mixtures better the COP of HTHP?
- How does the composition of these mixtures affect the exergy performance of HTHP?

**Table 1**  
Investigated mixtures in literature.

Reference	Working fluids (mixtures)	Method	Source Temp (°C)	Supply Temp (°C)
Gómez-Hernández et al. [37]	CO <sub>2</sub> /acetone	Theoretical	130	150–220
Navarro-Esbri et al. [38]	R1233zd(E)/R1336mzz(Z), R1233zd(E)/R1234ze(Z), R1233zd(E)/R601, R1234ze(Z)/R1336mzz(Z), R1234ze(Z)/R601, R1336mzz(Z)/R601	Theoretical	70	140
Zhang et al. [39]	BY-5	Experiment	70–80	110–130
Yan et al. [40]	DME/R134a, R152a/R1311, R290/R236fa, R290/R236ea, R600/R134a, R600/R152a, R600a/R134, R600a/R152a, R600a/R236fa, R600a/R245fa, R245fa/R600, R1311/R134, R1311/R290, R1311/R1234ze(E), R1234ze(Z)/R134, R1234ze(Z)/R600a, R245fa/R1233zd(E), R245fa/R142b, R245fa/R152a, R245fa/R161, R245fa/R236fa, R245fa/R600, R245fa/R600a, R600/R245fa	Theoretical	20	70–110
Xu et al. [35]	R245fa/R1233zd(E), R245fa/R142b, R245fa/R152a, R245fa/R161, R245fa/R236fa, R245fa/R600, R245fa/R600a, R600/R245fa	Experiment	45–65	80–100
Pan et al. [41]		Experiment and Theoretical	30–55	60–100
Wu et al. [20]	propylene/R601a, propane/R601a, propylene/R601, propylene/hexane, propane/hexane	Theoretical	15	15–90
Fernández-Moreno et al. [28]	R-515B	Theoretical	7.5–22.5	55–85
Kristensen et al. [42]	propylene/R600a, propylene/R600, propane/R600, CO <sub>2</sub> /propane, dimethyl ether/Isopentane	Theoretical	40	85
Zühlsdorf et al. [23]	CO <sub>2</sub> /dimethyl ether, dimethyl ether/R601a, dimethyl ether/R600, CO <sub>2</sub> /dimethyl ether, Ethane/propane, propylene/R600, ethane/propylene, propylene/R600, propane/R600, dimethyl ether/R601, dimethyl ether/R601a	Theoretical	40	80
Zhang et al. [43]	dimethyl ether/R744	Theoretical	20	65
Dai et al. [26]	CO <sub>2</sub> /R32, CO <sub>2</sub> /R41, CO <sub>2</sub> /1270, CO <sub>2</sub> /R290, CO <sub>2</sub> /R161, CO <sub>2</sub> /RE170, CO <sub>2</sub> /	Theoretical	30	60

(continued on next page)

Table 1 (continued)

Reference	Working fluids (mixtures)	Method	Source Temp (°C)	Supply Temp (°C)
	R152a, CO <sub>2</sub> / R1234yf CO <sub>2</sub> /R1234zeE, CO <sub>2</sub> /R134a			

- To what degree do the operating parameters affect the performance of HTHP?

## 2. Methods

### 2.1. HTHP model

The vapor compression cycle with internal heat exchanger (IHX), is utilized for this study. The configuration as presented in Fig. 1, is made up of five components; condenser, evaporator, compressor, expansion valve and internal heat exchanger (IHX). The modelling and analysis of the cycle configuration was done using the Aspen Plus V12.1 version [45,46]. The state of the fluid at the various points was calculated by the software using the REFPROP fluid property data base [47]. The condenser is modelled to be an all in one component, to take care of desuperheating, condensing and subcooling requirements of the cycle. The boundary conditions and input parameters are presented in Table 2. The heat source and sink were modelled as pressurised water, to keep the water in liquid state. The evaporation and condensation pressures were calculated at an evaporator and condenser minimum pinch point temperature difference ( $\Delta T_{pp}$ ) of 5 K. The mass flow rate of the working fluid was calculated for a condenser heat duty of 20 kW. Neglecting any form of losses, energy and mass balances were calculated for the components based on first and second law of thermodynamics using the simulation software packages for the various components (see section 2.3)

The working principle of the modelled cycle is shown in the flow and  $T,s$ -diagram in Fig. 1. Heat is transferred to the working fluid from the heat source to completely evaporate it to saturated vapor state as it leaves the evaporator at point 1. Flowing through the internal heat exchanger (IHX) it is heated to a superheated state at point 2 by the returning fluid from the condenser. The compressor then forces the fluid to a high pressure at point 3. In the condenser, the fluid is desuperheated to the saturated vapor state at point 4, condensed to the saturated liquid state at point 5 and then subcooled to point 6, while transferring heat to the heat sink. The fluid is further subcooled in the IHX to point 7 transferring heat to the other section of the IHX. With the help of the

Table 2  
Boundary conditions and model input.

Parameters	Constant value	Range
Heat source inlet temperature	50 °C	
Heat source outlet temperature	45 °C	
Heat source glide	5 K	5–20 K
Heat sink inlet temperature	80 °C	
Heat sink outlet temperature		140–170 °C
Heat source pressure	5 bar	
Heat sink pressure	15 bar	
Mole fraction (varied in 10 % steps)		0–1
Evaporator minimum pinch point temperature difference	5 K	
Condenser minimum pinch point temperature difference	5 K	
IHX minimum pinch point temperature difference	10 K	10–30 K
Degree of subcooling at condenser	10 °C	

expander, the fluid is expanded back to its low pressure and temperature at point 8 before entering the evaporator for a continuous cycle. Fig. 2 presents the flow chat that summarizes the methodology of the study.

#### 2.1.1. HTHP simulation in Aspen Plus

The selected model blocks for the various components as presented in Table 4 are connected with streams to depict the vapor-compression heat pump cycle as seen in Fig. 1. The Heatx block used for the heat exchangers has one degree of freedom where the degree of subcooling, vapor fraction at the cold side outlet and degree of superheating on the cold side of 10 °C, 1 and 10 K was specified for the condenser, evaporator and IHX respectively. Also, with the help of the built-in zone analysis feature, the heat exchangers were divided into 100 zones to enable a more accurate calculation of the minimum pinch temperature difference. For the expansion valve and isentropic compressor blocks, with one degree of freedom each, estimated exit pressures were provided. Using the design specification function, block input variables were manipulated to obtain the desired boundary conditions presented in Table 2, with a tolerance error of 0.01.

#### 2.2. Source and supply temperature selection

A range of 140–170 °C supply temperature was selected for this study. This range of supply temperature covers the required temperature of process heat for a wide range of applications in the metal, paper, chemical and food industries [48]. Also, high-temperature heat pumps with supply temperatures between 90 and 130 °C are already available in the market [22,49]. To provide heat at temperatures higher than 130 °C, novel concepts and working fluids must be investigated. Heat

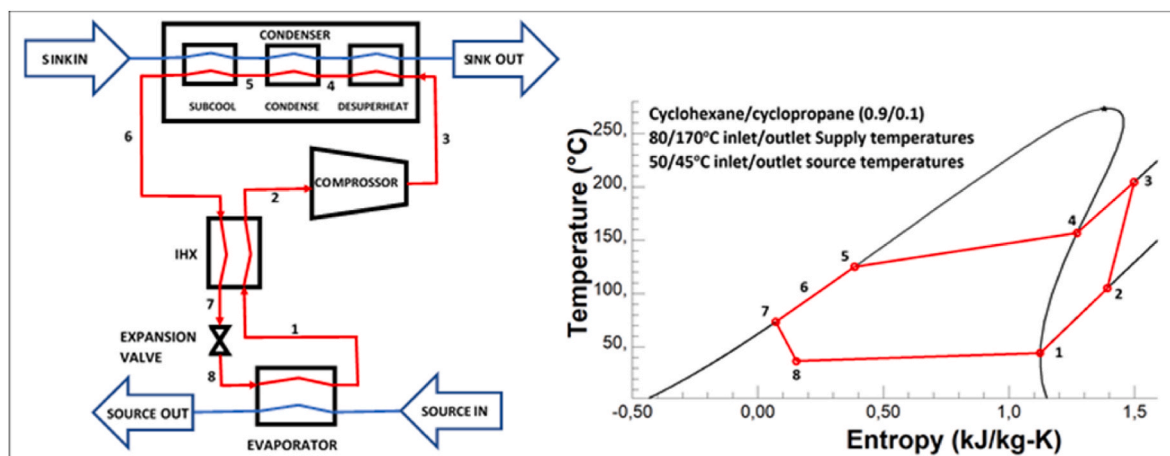


Fig. 1. Principle plant scheme of a heat pump flow (left side) and corresponding  $T,s$ -diagram (right side) for a zeotropic mixture as working fluid.

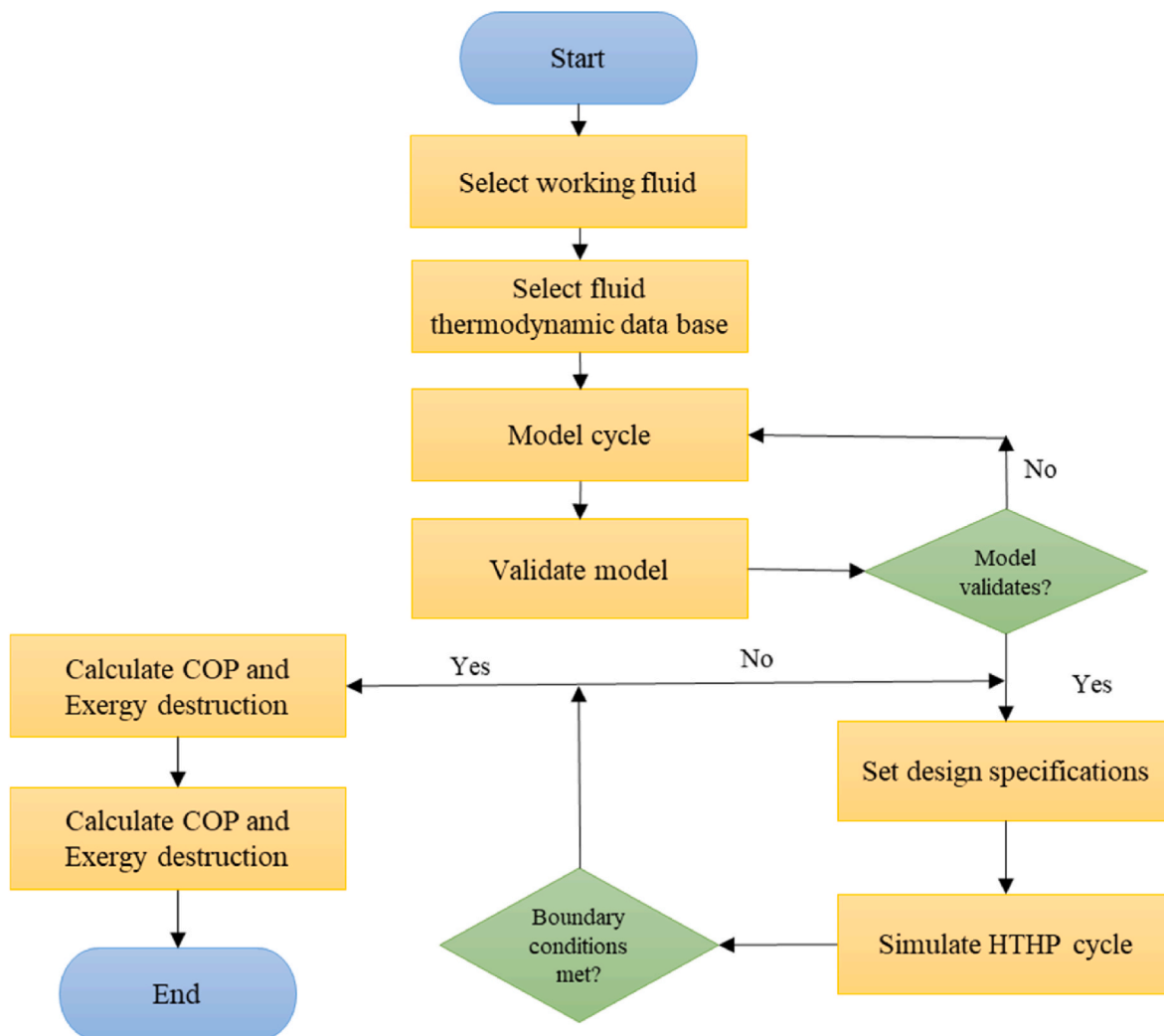


Fig. 2. Methodology flow chat.

source at 50 °C is typical for industrial waste heat recovery and medium-depth geothermal resources, which are the main sources of heat suitable for the integration of HTHPs in industrial applications. As alternative energy sources, these heat sources are noted for their major role in increasing energy efficiency and sustainability [50–52].

### 2.3. Working fluid selection

With the aim of providing high temperatures between 140 °C and 170 °C, two categories of potential fluids were selected. Hexamethyldisiloxane (MM), cyclohexane and cyclopentane (high critical

temperatures above 200 °C), were considered as the base constituent of all the mixtures studied. The application of this class of substances is one of the novel aspects of this study. The second category of mixture components comprised four hydrocarbons and three synthetic fluids with critical temperatures between 100 °C and 200 °C. These pure fluids are chosen according to existing literature. Table 3 presents the thermodynamic properties including ozone depletion potential (ODP), global warming potential (GWP), normal boiling point (NBP), critical temperature (CT), critical pressure (CP) and safety class of the selected fluids. The ODP and GWP of the fluids were obtained according to the Intergovernmental Panel on Climate Change (IPCC) fourth assessment

**Table 3**  
Properties of selected fluids.

Fluids	Type	ODP	GWP (100-yr)	NBP (°C)	CT (°C)	CP (bar)	Safety Class
Hexamethyldisiloxane (MM)	Siloxane	–	n.a.	100.0	245.6	19.3	n.a.
Cyclohexane	HC	0	n.a.	80.7	280.7	40.8	A3
Cyclopentane	HC	0	n.a.	49.3	238.6	45.1	A3
Butane (R600)	HC	0	<1	–0.5	152.0	38.0	A3
Isobutane (R600a)	HC	0	<1	–11.7	134.7	36.4	A3
Pentane (R601)	HC	0	<1	36.1	196.6	33.6	A3
Isopentane (R601a)	HC	0	<1	27.7	187.8	33.8	A3
Cyclopropane	HC	0	86	–32.8	124.9	55.4	A3
R1336mzz(Z)	HFO	0	2	37.4	171.3	29.0	A1
R1234ze(Z)	HFO	0	6	9.4	150.1	35.3	A2L
R1233zd(E)	HCFO	0.00034	1	17.9	165.5	35.7	A1

report and the 2022 scientific assessment on ozone depletion report of World Meteorological Organization (WMO). [53,54], while the other properties were obtained from REFPROP version 10 data base [47].

### 2.3.1. Working fluid selection criteria

The choice of working fluids is informed by a few factors which cut across environmental, safety and application factors. The environmental factors considered are the ozone depletion potential (ODP) and global warming potential (GWP), while the safety class covers the toxicity and flammability of the fluids. In numerous publications fluid selection for low and high temperature ORC systems has been conducted. In parallel to heat pumps, refrigerants like HFCs or natural hydrocarbons are limited to certain process temperatures [55–57]. For high temperature applications long-chained hydrocarbons or siloxanes are more suitable [58–60]. Regarding mixtures, previous studies have already proven the potential increase of efficiency for heat pump and ORC systems with a good glide match at phase change. This study intends to apply the analogy of fluid selection in organic Rankine cycle (ORC) to heat pumps. Thus, the criteria for the fluid selection is summarized.

- GWP < 100 and very low ODP.
- Critical temperatures: medium CT ( $100^{\circ}\text{C} < x < 200^{\circ}\text{C}$ ), high CT ( $> 200^{\circ}\text{C}$ ).
- Fluids already applied to medium and high temperature ORC.

### 2.4. Energy and exergy analysis

Mass and energy balances were performed for the various components by the Aspen Plus simulation software using built in thermodynamic models for the selected component packages. The chosen model blocks in the simulation software are presented in Table 4.

The coefficient of performance (COP) of the system is given as

$$COP = Q_{Cond} / W_{Comp} \quad (1)$$

where  $Q_{Cond}$  is the heat transferred in the condenser and  $W_{Comp}$  is the required compressor power. The heat transferred in the condenser is calculated from the state points of the system and it is as

$$Q_{cond} = \dot{m}(h_3 - h_6) \quad (2)$$

where  $\dot{m}$  is the mass flow rate of the system,  $h_3$  and  $h_6$  are the enthalpy at point 3 and 6, respectively. Also, the required electric power input to the compressor is given as

$$W_{comp} = \dot{m}(h_{3s} - h_2) / \eta_{is} \quad (3)$$

$h_{3s}$  is the isentropic enthalpy at point 3 and  $\eta_{is}$  is the isentropic efficiency of the compressor, which is chosen to be 72 %. The chosen isentropic efficiency is the default compressor isentropic efficiency in Aspen plus and it falls within the range of published testing results [8].

The importance of exergy analysis in high-temperature heat pump design cannot be undermined. This is because optimizing the compo-

**Table 4**  
Selected model blocks.

Components	Model blocks	Thermodynamic model	Reason
Evaporator, IHX and condenser	HeatX	$\dot{Q} = \dot{m}C_p\Delta T$	Calculates the required duty surface area and heat transfer coefficients in the counter-current direction.
Compressor	Isentropic compressor	$\eta_{is}(h_3 - h_2) = (h_{3s} - h_2)$	Calculates the required power for isentropic compression
Expansion valve	Valve block	$\Delta h = 0$	Calculates pressure drop

nents of the system is largely dependent on how much the exergy destruction in that component is reduced. For a system with many components, the exergy destruction is the sum of the exergy destruction in individual components of the system [61]. Thus, total exergy destruction is given as

$$e_{d(total)} = e_{d(Evap)} + e_{d(IHX)} + e_{d(Comp)} + e_{d(Cond)} + e_{d(Exp)} \quad (4)$$

The exergy destruction is a function of flow exergy which is the difference in terms of the availability of flow of a stream in comparison to its dead state given as;

$$e_d = (h - T_o s) - (h_o - T_o s_o) \quad (5)$$

Combining the flow exergy equation with energy balance equation, the exergy destruction for the various components is deduced and presented in Table 5.  $m_{so}$  and  $m_{si}$  represent the mass flowrate at the source and sink, respectively.

### 3. Validation of model

For validation purposes, the applied model is adapted to literature scenarios in order to ascertain the level of accuracy and stable performance. Tables 6 and 7 present the validation of the developed model with existing results, both for pure fluids and mixtures. Bamigbetan et al. [6] modelled a heat pump with  $60^{\circ}\text{C}$  heat source temperature,  $80^{\circ}\text{C}$  heat sink inlet temperature and  $100^{\circ}\text{C}$  heat sink outlet temperature. The working fluids were superheated by 10–15 K at the evaporator and the system has a capacity of 20 kW. By Zühlsdorf et al. [23], the heat exchangers were modelled to have a minimum pinch temperature difference of 5 K, heat sink inlet and outlet temperatures of  $40^{\circ}\text{C}$  and  $80^{\circ}\text{C}$  respectively and a minimum superheating of 5 K at the evaporator. The heat source outlet temperatures are  $35^{\circ}\text{C}$  for R600, R600a and R601;  $25^{\circ}\text{C}$  for 30%R1270-70%R600, 30%R290-70%R600, and 80% RE170-20%R601a;  $20^{\circ}\text{C}$  for R601a and 30%RE170-70%R601. It can be seen that the relative mean deviation is below 2.12 % for all considered cases. This proves the sufficient accuracy of the applied simulation model.

### 4. Results and discussion

This section presents the findings on the investigated fluid mixtures. The performance of the pure fluids is first analysed and compared. The performance of the mixtures of the three high critical temperature fluids with R601a is evaluated and best performing high critical temperature fluid selected for further analysis. The effect of various operating parameters is also investigated and presented in this section.

#### 4.1. Performance of pure fluids

The COP and pressure ratio as a function of supply temperature for the pure fluids are presented in Fig. 3. Cyclohexane shows the highest performance among the high critical temperature fluids. For the lower critical temperature fluids, cyclopropane leads to the highest COP. For supply temperatures above  $150^{\circ}\text{C}$ , cyclopropane records a 1.82 % higher COP than cyclohexane. With the low critical temperature limitation of cyclopropane, such high supply temperatures can only be

**Table 5**  
Expression for exergy destruction in the various components.

Component	Exergy destruction equation
Evaporator	$e_{d(evap)} = \dot{m}(\dot{E}X_8 - \dot{E}X_1) + m_{so}(\dot{E}X_9 - \dot{E}X_{10})$
IHX	$e_{d(IHX)} = \dot{m}(\dot{E}X_1 - \dot{E}X_2) + \dot{m}(\dot{E}X_6 - \dot{E}X_7)$
Compressor	$e_{d(comp)} = W_{comp} - \dot{m}(\dot{E}X_3 - \dot{E}X_2)$
Condenser	$e_{d(cond)} = \dot{m}(\dot{E}X_5 - e_{d6}) + m_{si}(\dot{E}X_{11} - \dot{E}X_{12})$
Expansion valve	$e_{d(Exp)} = \dot{m}(\dot{E}X_7 - \dot{E}X_8)$

**Table 6**  
Model validation for pure fluids.

Fluid	COP		Relative mean deviation (%)
	Previous Studies	Present Model	
R600	5.38 [23] 3.3 [6]	5.33 3.23	0.93 2.12
R600a	5.34 [23] 3.0 [6]	5.31 3.03	0.56 1.0
R601	4.91 [23] 3.4 [6]	4.88 3.44	0.61 1.17
R601a	4.41 [23] 3.4 [6]	4.36 3.39	1.13 0.3
R1336mzz (Z)	3.3 [6]	3.26	1.21
R1234ze(Z)	3.4 [6]	3.45	1.47
R1233zd(E)	3.4 [6]	3.47	2.06

**Table 7**  
Model validation for mixtures.

Mixtures	COP		Relative mean deviation (%)
	Previous Studies	Present Model	
30%R1270-70% R600	5.40 [23]	5.41	0.19
30%R290-70% R600	5.38 [23]	5.42	0.74
80%RE170-20% R601a	5.31 [23]	5.35	0.75
30%RE170-70% R601	5.24 [23]	5.15	1.72

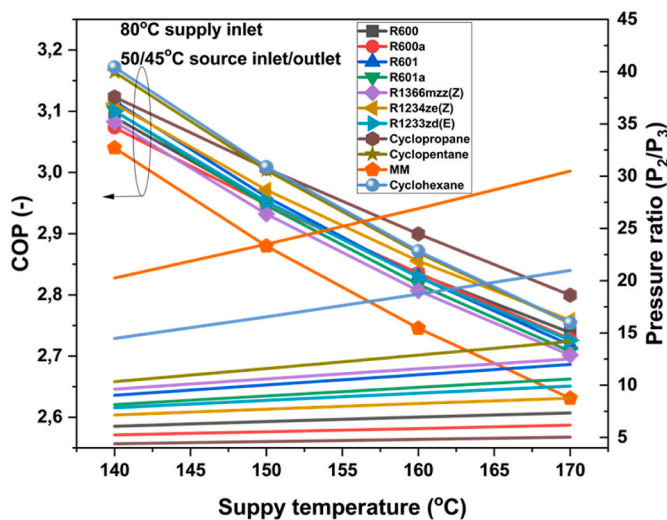


Fig. 3. COP of pure fluids depending on supply temperature.

achieved in supercritical operations. MM is seen to be the least performing fluid with a COP of about 2.5 at a supply temperature of 170 °C.

One other major issue with the use of MM is its high pressure-ratio as seen also from Fig. 3, which is actually a major contributor to its lower performance in comparison to other fluids. The compressor heat pump with MM as working fluid must be able to compress the fluid over a pressure ratio of 30 for 170 °C supply temperature. However, for such a high pressure ratio, multi-stage compression is required, thus incurring higher equipment cost. Cyclopentane shows good prospects among the higher critical temperature fluids with its COP slightly lower than that of cyclohexane.

4.2. Performance of mixtures

4.2.1. COP as a function of mixture composition

COP as a function of mole fraction for the mixtures of the high critical temperature fluids with R601a is presented in Fig. 4. The graphs clearly show that the mole fraction of the fluids affects the system performance. From the obtained result for MM mixtures, the COP obtained for the different mole fractions is less than that for pure MM. This shows that MM does not have suitable temperature glide matching in the heat exchanger with the considered fluids. For cyclopentane mixtures, higher COPs are clearly seen especially at higher mole fraction of cyclopentane indicating a suitable temperature glide matching in the heat exchanger. 1.42 % increase in COP is recorded at 0.8 mol fraction of cyclopentane for this mixture. A higher performance is recorded, however, by the cyclohexane mixture, with a 2.85 % increase in COP compared to pure cyclohexane. The disparity in the curves of cyclohexane/R601a and cyclopentane/R601a is due to the difference in the evaporation and condensation temperature glide of these mixtures. Cyclohexane/R601a has a much higher evaporation temperature glide compared to cyclopentane/R601a. Higher temperature glide during phase changes indicates a high mismatch of the mixture composition in the heat exchanger [23]. Due to the relatively lower temperature glide throughout the composition of cyclopentane/R601a, a smooth curve is observed with no minimum, indicating a good match throughout the compositions, but no competitive COP increase compared to Cyclohexane/R601a. With good glide matching obtained for cyclohexane, it will be selected for further analysis as the base fluid in the mixture with other lower critical temperature fluids.

More comprehensive simulation results for the mixture of cyclohexane and lower critical temperature fluids depending on the mole fraction are presented in Fig. 5 for the case of 140 °C supply temperature. A repetition of the performance increase can be seen for mixtures of cyclohexane with lower critical temperature fluids. The highest performance is evidently at 0.9 mol fraction of cyclohexane for all the mixtures. A COP of 3.34 is recorded by the cyclohexane/cyclopropane mixture, which accounts for a 5.23, 6.88, 7.71 and 7.74 % increase from

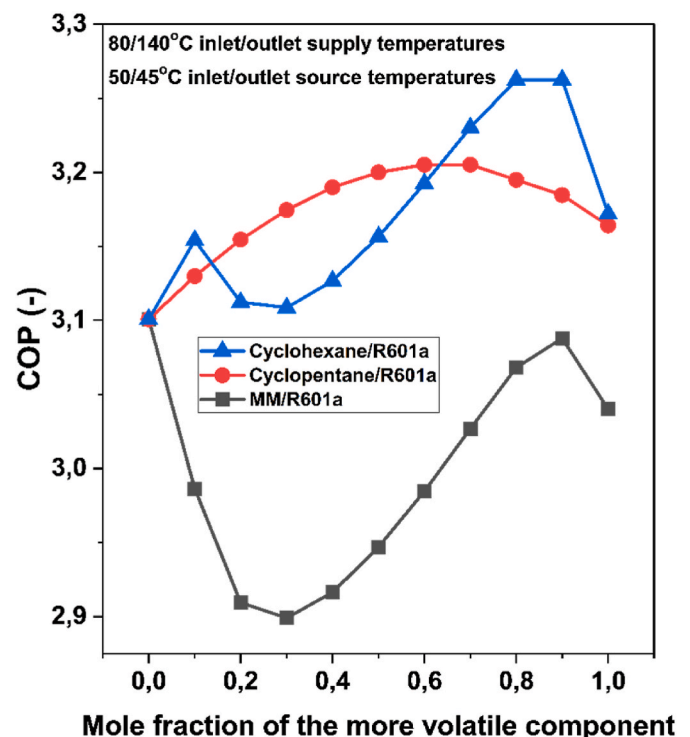


Fig. 4. COP for high critical temperature fluid mixtures with R601a.

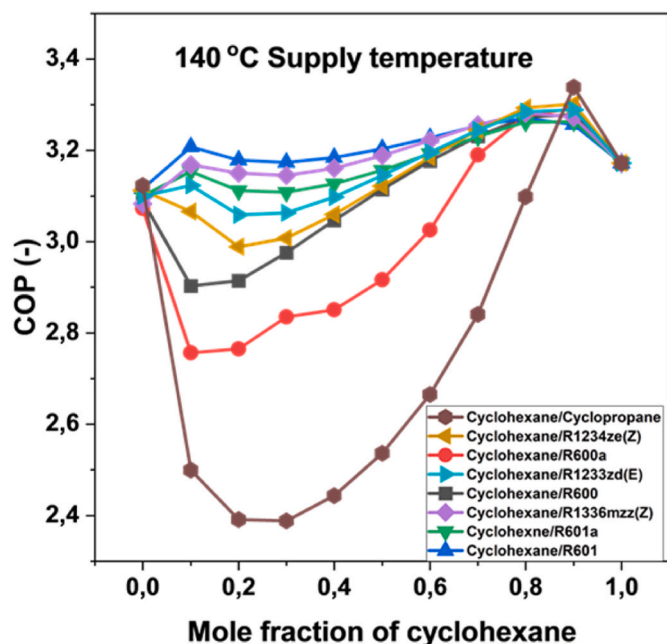


Fig. 5. COP as a function of mixture composition.

the COP of pure cyclohexane, cyclopropane, R1233zd(E) and R601a respectively. The mixtures of R601, R1336mzz(Z) and R601a should be noted for their generally sufficient temperature glide matching. The temperature glide of the mixtures in the heat exchangers are discussed in section 4.3. Every mole fraction of these three mixtures has COP higher than those of its pure fluid constituent. For the other fluid mixtures, composition with insufficient temperature glide matching can be clearly seen with lower COPs.

#### 4.2.2. Temperature glide matching as a function of mixture composition

Unlike pure fluids, the evaporation and condensation of zeotropic mixtures occur in a temperature glide. Fig. 6 presents the graph of evaporation temperature glide as a function of mole fraction for the various mixtures.

The evaporation temperature glide as a function of mole fraction is presented in Fig. 6. It illustrates the nature of the temperature glide matching of the mixtures at the evaporator. As the temperature glide

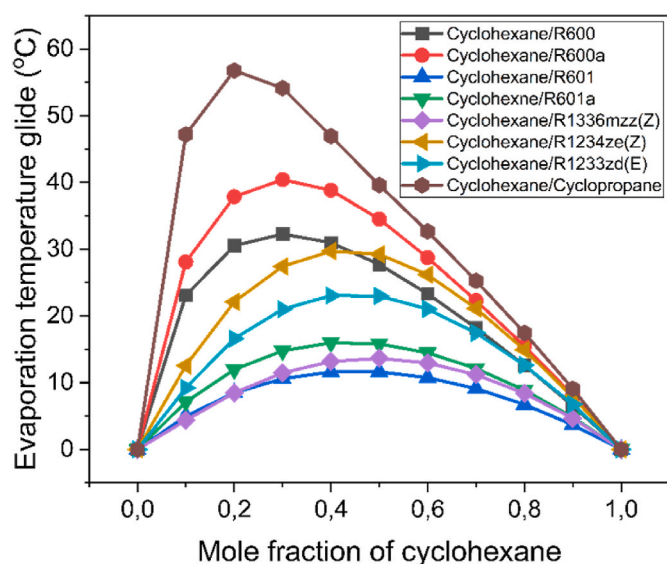


Fig. 6. Evaporation temperature glide as a function of mole fraction.

deviates from the temperature difference of the heat source, the increase in efficiency becomes less pronounced. This is typical for the case of cyclohexane/cyclopropane, cyclohexane/R600a, cyclohexane/R600 and cyclohexane/R1234ze(Z) mixtures with high evaporation temperature glides. However, it can also be said for the design conditions that mixture compositions with evaporation temperature glide around 10 °C exhibit a more pronounced COP increase. The heat exchangers at the heat source and sink gives us a clear picture of the nature of the temperature glide match of a mixture [23]. Fig. 7 presents the heat transfer curves at the evaporator and condenser for two compositions of cyclohexane/cyclopropane mixture at 140 °C supply temperature. For the cyclohexane/cyclopropane (0.9/0.1) mixture, a more suitable glide match is seen at the evaporator than in the condenser, with the two curves very close to each other. This explains the reduced exergy destruction of 0.25 kW at the evaporator compared to 0.77 kW at the condenser.

In the case of the cyclohexane/cyclopropane (0.2/0.8) mixture both the evaporator and condenser record a less sufficient temperature glide match, leading to increased irreversibility (exergy destruction), in this case 34.4 % and 11.8 % higher than that of cyclohexane/cyclopropane (0.9/0.1) mixture for the evaporator and condenser respectively. Similar trends are also seen across the mixtures and supply temperatures, which goes to prove the importance of exergy analysis in thermodynamic systems [62].

#### 4.2.3. Evaporation temperature as a function of mixture composition

One of the main thermodynamic issues with the use of cyclohexane as a pure working fluid for low temperature heat sources is its high normal boiling point, which results in a low evaporation pressure. Very low evaporation pressures lead to safety concerns especially for flammable fluids [6]. From Fig. 8, the evaporation pressure is seen to increase with the addition of the lower boiling point fluids. With just 0.1 mol fraction of the lower boiling point fluids, the evaporation pressure increases beyond 0.3 bar, which has already been reported in existing systems. With these increasing evaporation pressure effect, the flammability of HFO-mixtures like that of R1233zd(E) might be suppressed [63].

#### 4.2.4. Critical temperature and pressure as a function of mixture composition

For a higher supply temperature, the critical temperature and pressure of working fluids are of utmost importance to avoid supercritical operations. Fig. 9 shows the critical temperature and pressure as a function of mole fraction. The presence of high critical temperature fluids like cyclohexane makes it possible for lower critical temperature fluids such as R600a (with a critical temperature less than 140 °C) to attain a mixture with a critical temperature as high as 250 °C. For other considered fluids like R601 (with 196 °C critical temperature), mixtures with critical temperatures as high as 270 °C were obtained. With these obtained high critical temperatures, the supply temperature considered in this work, falls within the subcritical operation, as seen in Fig. 9. This same trend is also for the critical pressure. However, with cyclopropane having a higher critical pressure than cyclohexane it can be seen that cyclohexane/cyclopropane mixtures lead to a higher critical pressure than that of pure hexane. These obtained critical pressures are above the pressures considered in this study (see Fig. 10).

### 4.3. Influence of operating parameters

#### 4.3.1. Effect of supply temperature on COP

The COP for the zeotropic mixtures of cyclohexane as a function of mole fraction and selected supply temperatures between 140 °C and 170 °C are presented in Fig. 11. Mixtures with suitable temperature glide matching in the heat exchanger are seen with higher COPs relative to the pure fluids. For the mixtures of R601, R1336mzz(Z), R601a and R1233zd(E), COP graphs with two peaks are seen. This graph pattern is

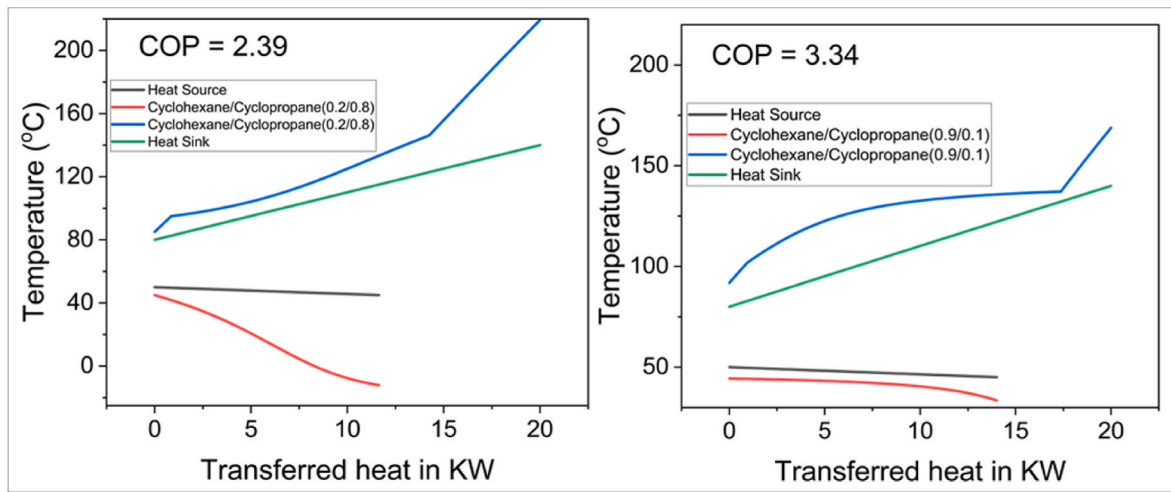


Fig. 7. Temperature-enthalpy flow-diagram for cyclohexane/cyclopropane mixtures at 140 °C supply temperature.

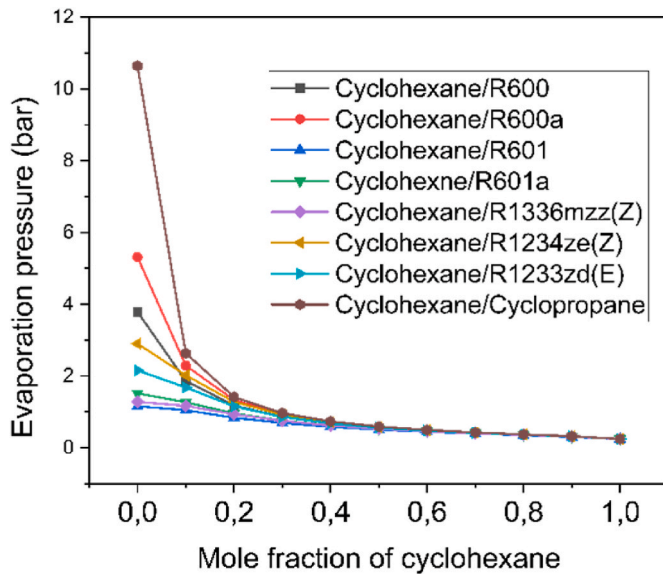


Fig. 8. Evaporation pressure depending on mixture composition.

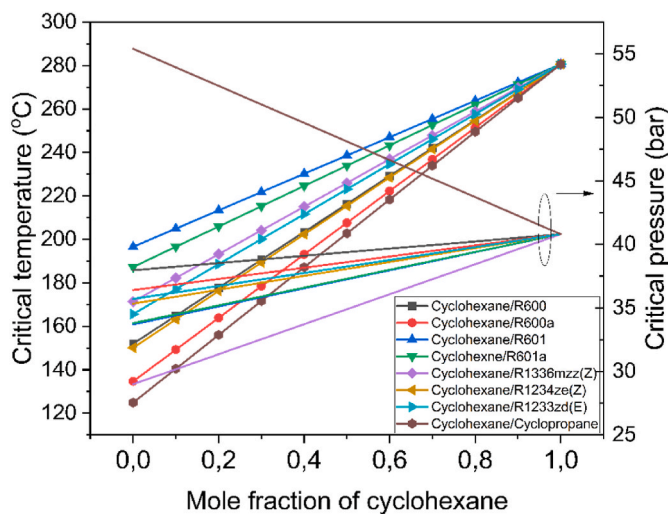


Fig. 9. Critical temperature and pressure depending on mixture composition.

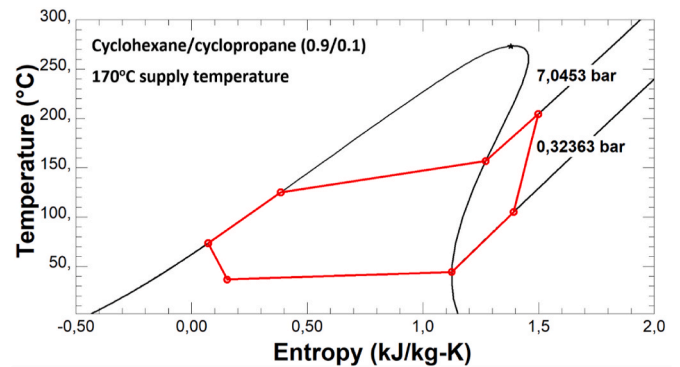


Fig. 10. T-s diagram for cyclohexane/cyclopropane (0.9/0.1) mixture.

similar to those obtained in other studies [20,23,24,42]. For the other fluid mixtures, a decreasing trend can be seen at the initial addition of cyclohexane. This sharp decrease is even more pronounced for the cyclopropane mixture which is actually the fluid with the lowest boiling point and consequently highest critical temperature difference from cyclohexane. The highest COP obtainable by the mixtures remained consistent at the mole fraction of 0.9 cyclohexane, across all the supply temperatures considered. The obvious dominance of the higher critical temperature fluid for high COP is consistent with the result obtained in previous studies [23,28,42]. Cyclohexane/R1234ze(Z) is seen to be higher in efficiency than other HFO-mixtures, with that of cyclohexane/R1233zd(E) closely following. The most efficient mixture is cyclohexane/cyclopropane (0.9/0.1), with COP between 3.34 and 2.81 for supply temperatures between 140 and 170 °C. This actually increased the COP of pure cyclohexane and cyclopropane by 5.36 % and 7.05 % respectively for 140 °C supply temperature. However, the least performing mixture, cyclohexane/R601 also recorded an increase of 2.71 % and 4.69 % in COP from that of pure cyclohexane and R601 respectively.

#### 4.3.2. Effect of supply temperature on compressor suction and discharge temperatures

The effect of high supply temperature is a challenge for the compressor components [6], due to the fact that the highest temperature in the cycle is recorded at the exit of the compressor. Hence this temperature is a design criterion that must be put into consideration in the design of compressors for different supply temperatures. Fig. 12 shows the compressor discharge and suction temperature as a function of

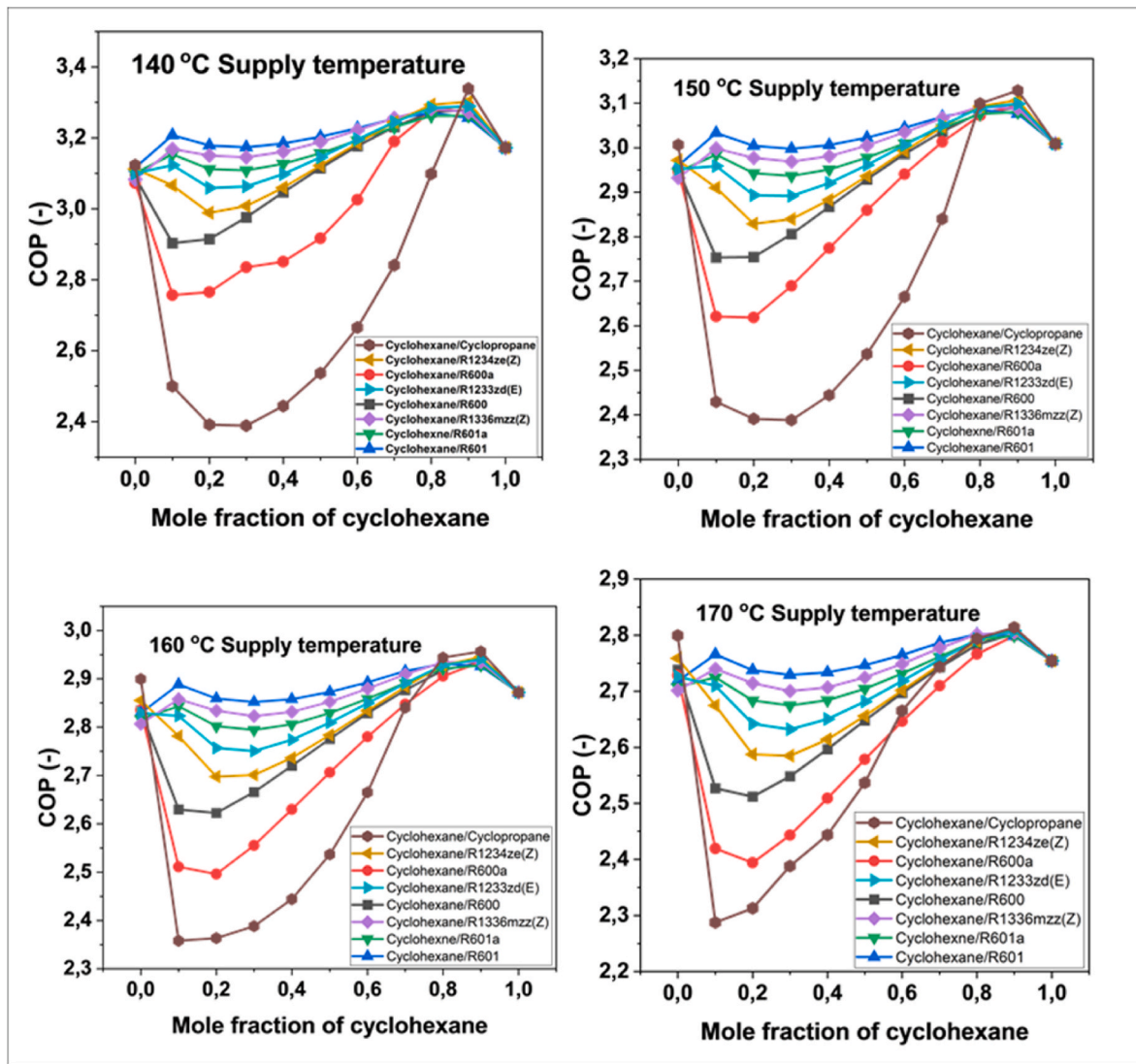


Fig. 11. COP of cyclohexane mixtures as function of supply temperature.

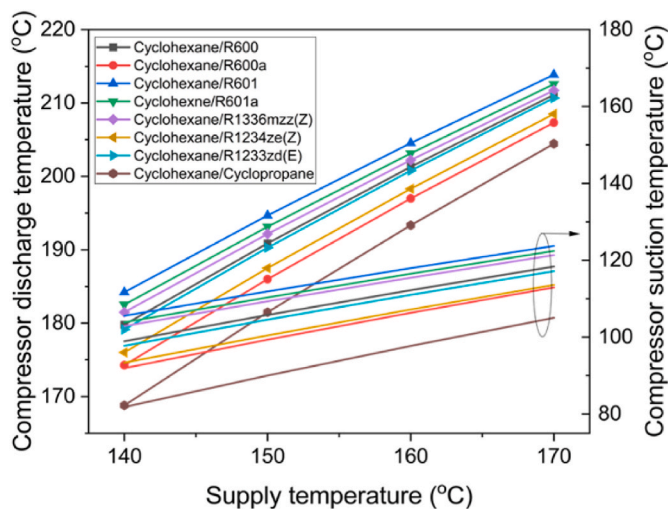


Fig. 12. Compressor suction and discharge temperatures at varying supply temperatures.

supply temperature at 0.9 mol fraction of cyclohexane. The

cyclohexane/R601 mixture recorded the highest discharge temperature of 213.86 °C and 184.21 °C for 170 °C and 140 °C supply temperatures, respectively. The compressor suction temperature also follows the same trend for the various mixtures. The cyclohexane/cyclopropane mixture recorded a lower compressor suction and discharge temperatures of 104.99 °C and 204.44 °C respectively at 170 °C supply temperature. These temperatures however must be kept in check in the design of the compressor components [8]. The key performance indicator for the investigated fluids is presented in Table 8.

#### 4.3.3. Effect of heat source temperature difference on COP and exergy destruction

COP and total exergy destruction as a function of heat source temperature difference are presented in Fig. 13. An increase in the heat source temperature difference is seen to have a negative effect on the performance of the heat pump. At 140 °C supply temperature, a 15 K increase in heat source temperature difference decreases the COP of the cyclohexane/cyclopropane mixture by 4.32 %. A larger decrease of 12.32 % is recorded with the cyclohexane/R601 mixture. However, at 170 °C supply temperature, the effect is higher with a resultant 7.5 % decrease in COP for cyclohexane/cyclopropane mixture. This negative effect is due to the decreasing evaporation pressure, resulting in a higher pressure ratio and compressor work requirement [11]. The obtained

**Table 8**  
Key performance indicator for investigated fluids at 170 °C supply temperature.

Fluids	COP (-)	Pressure Ratio (-)	Compressor exit temperature (°C)	Mass flowrate (kg/s)
Cyclohexane/Cyclopropane (0.9/0.1)	2.814	21.8	204.4	0.040
Cyclohexane/R1234ze(Z) (0.9/0.1)	2.810	20.4	208.5	0.444
Cyclohexane/R1233zd(E) (0.9/0.1)	2.808	19.8	210.7	0.044
Cyclohexane/R1336zz(Z) (0.9/0.1)	2.805	19.4	211.7	0.046
Cyclohexane/R600 (0.9/0.1)	2.802	19.6	211.1	0.041
Cyclohexane/R601a (0.9/0.1)	2.799	19.1	212.6	0.042
Cyclohexane/R600a (0.9/0.1)	2.799	20.5	207.3	0.041
Cyclohexane/R601 (0.9/0.1)	2.799	19.1	213.9	0.042
Cyclopropane	2.800	5.0	204.4	0.045
R1234ze(Z)	2.759	8.7	208.8	0.088
Cyclohexane	2.754	20.0	219.1	0.041
Cyclopentane	2.754	14.2	227.0	0.040
R600	2.738	7.3	195.4	0.050
R600a	2.728	6.2	185.5	0.058
R1233zd(E)	2.726	9.9	211.7	0.094
R601	2.718	11.0	202.6	0.047
R601a	2.708	10.6	198.1	0.051
R1336zz(Z)	2.702	12.5	197.7	0.108
MM	2.631	30.5	187.9	0.077

result is consistent with findings in literature [23,24]. Also, from Fig. 13, increasing the heat source temperature difference increases the total exergy destruction. The cyclohexane/R601 mixture recorded the highest exergy destruction increase of 14.94 %, while that of the cyclohexane/cyclopropane mixture increased by 8.55 %. This trend is in agreement with the findings of Yelishala et al. [24] in their study on zeotropic mixtures. The exergy destruction in various system components for the best performing mixture compositions is summarized in Table 9.

**4.3.4. Effect of the heat source temperature difference on evaporation pressure and pressure ratio**

One negative effect of increasing the heat source temperature difference is the decrease in the evaporation pressure. This can be clearly seen from Fig. 14. An average of 7 % decrease in the compressor pressure is recorded across the mixtures over the 15 K increase in the heat source temperature difference. This is due to the fact that increasing heat source temperature difference at constant heat source inlet temperature, decreases the evaporation temperature and consequently evaporation pressure, if the fluid must be completely vaporized at the exit of the evaporator. However, with this reduction in evaporation pressure, a corresponding increase in pressure ratio is seen due to an increasing difference between the evaporator and compressor pressures. This effect is also seen in Fig. 14.

**4.3.5. Effect of IHX pinch point temperature difference on COP and exergy destruction**

The effect of a varying minimum pinch temperature difference ( $\Delta T_{pp}$ ) of the internal heat exchanger (IHX) on the system performance was evaluated and presented in Fig. 15.

COP as a function of IHX pinch point temperature difference (IHX  $\Delta T_{pp}$ ) for 140 °C and 170 °C supply temperatures are presented in Fig. 12. It can be seen that an increase in the IHX  $\Delta T_{pp}$  decreases the

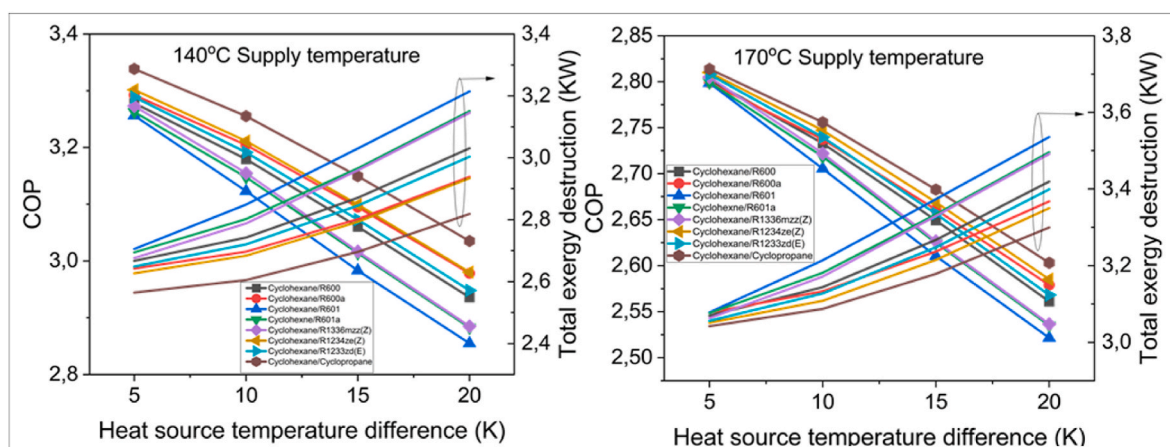


**Fig. 13.** COP and total exergy destruction at varying heat source temperature difference.

**Table 9**  
Exergy destruction in various system components.

Mixtures	Exergy destruction (kw) at 170 °C supply temperature				
	Evaporator	IHX	Compressor	Condenser	Expansion valve
Cyclohexane/Cyclopropane (0.9/0.1)	0.22	0.17	1.27	1.02	0.36
Cyclohexane/R1234ze(Z) (0.9/0.1)	0.22	0.21	1.26	1.07	0.30
Cyclohexane/R1233zd(E) (0.9/0.1)	0.21	0.23	1.26	1.10	0.27
Cyclohexane/R1336zz(Z) (0.9/0.1)	0.21	0.25	1.26	1.11	0.24
Cyclohexane/R600 (0.9/0.1)	0.21	0.23	1.26	1.10	0.27
Cyclohexane/R601a (0.9/0.1)	0.21	0.26	1.26	1.12	0.24
Cyclohexane/R600a (0.9/0.1)	0.22	0.21	1.27	1.07	0.32
Cyclohexane/R601 (0.9/0.1)	0.21	0.27	1.25	1.14	0.22

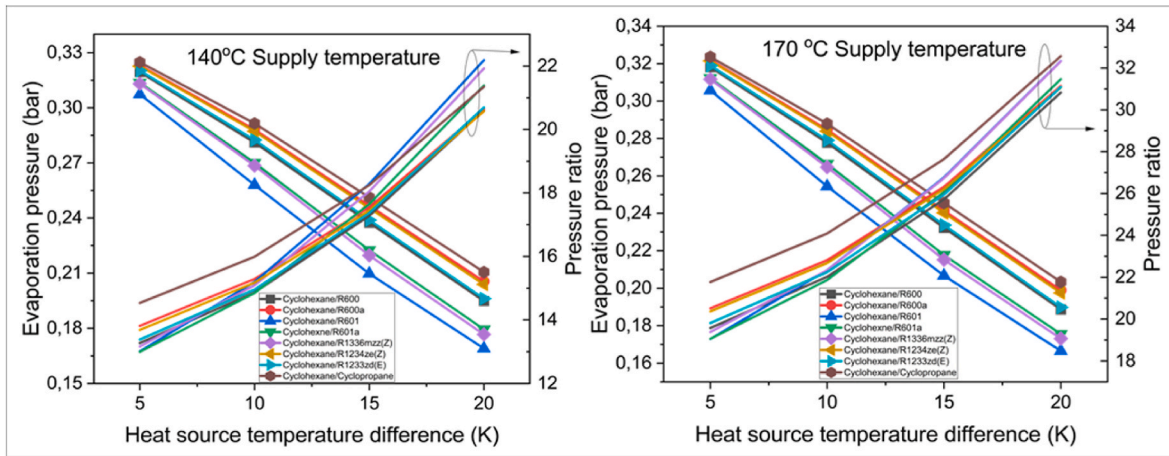


Fig. 14. Evaporation pressure and pressure ratio at varying heat source temperature difference.

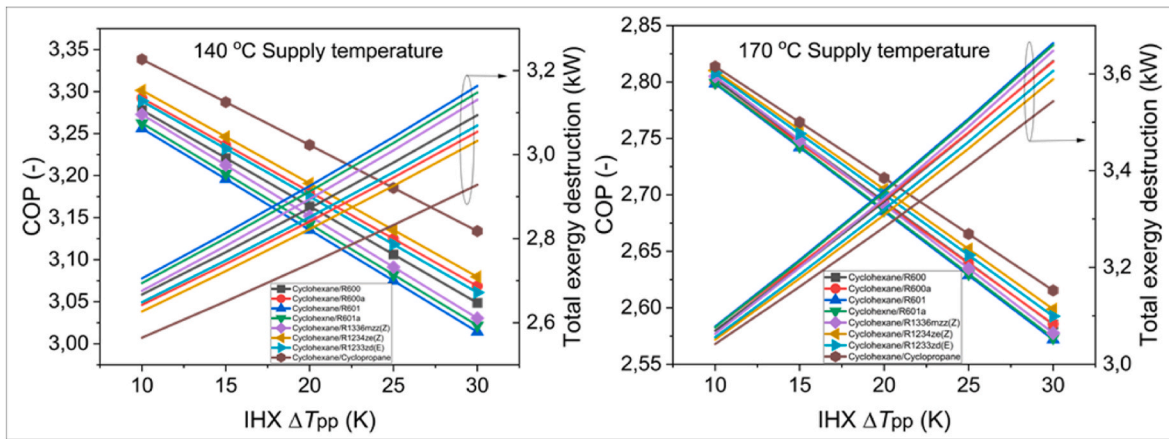


Fig. 15. COP and total exergy destruction at varying IHX  $\Delta T_{pp}$ .

COP. A 20 K increase in IHX  $\Delta T_{pp}$  decreased the COP of the cyclohexane/cyclopropane mixture by 6.29 %, for a 140 °C supply temperature. For a 170 °C supply temperature, increasing the IHX  $\Delta T_{pp}$  from 10 to 30 K results in an 8.07, 7.67 and 7.07 % decrease for R601a, R1233zd (E) and cyclopropane mixtures at 0.9 mol fraction of cyclohexane respectively. This decreasing COP effect is due to the fact that increasing  $\Delta T_{pp}$  reduces the quantity of heat transfer and hence reduces the

temperature of the fluid at the compressor suction. Moreover, from Fig. 15 a total exergy destruction is seen to increase with increasing IHX  $\Delta T_{pp}$ , which also contributes to the decrease in COP. The exergy destruction of the cyclohexane/cyclopropane mixture increased from 2.56 kW to 2.93 kW over the 20 °C increase in IHX  $\Delta T_{pp}$  at 140 °C supply temperature, while a 16.45 % increase was recorded at 170 °C supply temperature.

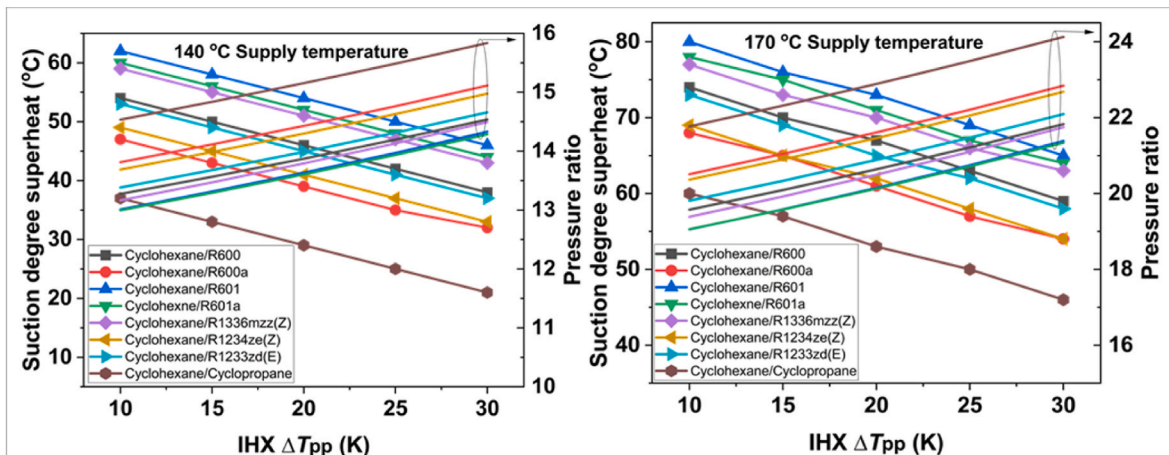


Fig. 16. Compressor suction degree superheat and pressure ratio at varying IHX  $\Delta T_{pp}$ .

#### 4.3.6. Effect of IHX pinch point temperature difference on evaporation pressure and pressure ratio

Research has proven that the addition of IHX increases the COP of heat pumps [21]. This is because the internal heat exchanger (IHX) increases the temperature and consequently the degree of superheat of the fluid at the compressor suction. This leads to less compressor work requirement to attain specific supply temperatures. Suction degree superheat and pressure ratio as a function of IHX  $\Delta T_{pp}$  is presented in Fig. 16. The compressor suction degree superheat of the cyclohexane/cyclopropane mixture decreased from 37 °C to 21 °C over the 20 K increase in IHX  $\Delta T_{pp}$ , at 140 °C supply temperature. At 10 K IHX  $\Delta T_{pp}$ , the suction degree superheat of the cyclohexane/cyclopropane mixture is at 60 °C for 170 °C supply temperature, which is the least among the considered mixtures. Increasing the IHX  $\Delta T_{pp}$  to 30 K reduces the degree superheat by 23.33 %. The opposite can be said concerning the IHX  $\Delta T_{pp}$  effect on the pressure ratio. The pressure ratio increased by 11.51 % at an IHX  $\Delta T_{pp}$  increase of 20 K for the cyclohexane/cyclopropane mixture at 0.9 mol fraction of cyclohexane for 170 °C supply temperature. This increase in pressure ratio contributes to the decrease in COP.

#### 4.4. Limitations of the study

Neglecting pressure and heat losses, is one of the main limitations of this study. For a more practical scenario these losses could constitute up to 10 % reduction in COP. In addition, the study is limited to a constant isentropic efficiency at the compressor which will rather reduce with increasing temperature lift as can be seen from many experimental studies. It should, however, be noted that the considered mixtures have not been experimentally proven. Thus, the obtained results are only valid from a simulation point of view. The compressor discharge temperatures obtained in this study are beyond the limit for commercially available compressors, thus placing a limitation to the application of the findings. With the high pressure-ratios obtained in this study, the use of multistage compressors will be more practical and safer. Finally, the evaporation pressures obtained in the study are below the atmospheric pressure, hence raising some safety concerns with the system.

#### 5. Conclusion

The thermodynamic analysis of working fluid mixtures of R600, R600a, R601, R601a, R1336mzz(Z), R1234ze(Z), R1233zd(E) and cyclopropane with cyclohexane have been theoretically conducted and the following conclusions are drawn.

- i. Cyclohexane/cyclopropane mixture at 0.9 mol fraction of cyclohexane has the highest COP of 2.81 for supply temperatures at 170 °C. This mixture improved the efficiency of the HTHP, with the obtained COPs higher than those of standard working fluids like R601a and R1233zd(E) by 7.16 and 7.19 % respectively at 140 °C supply temperature.
- ii. The degree of increase of performance of the HTHP using zeotropic mixtures depends on the temperature glide matching in the heat exchangers; as the temperature glide deviates from the temperature difference at the heat source or sink, the increase in efficiency becomes less pronounced.
- iii. Reduced exergy destruction accounts for an increase in efficiency, thus deliberate efforts must be made towards reducing exergy destruction if improved efficiency must be achieved.

#### Nomenclature

Comp Compressor

- iv. Boundary conditions such as the heat source temperature difference and the internal heat exchanger pinch point temperature difference (IHX  $\Delta T_{pp}$ ), have proven to affect the performance of the system. An increase in the heat source temperature difference from 5 to 20 K decreased the COP of the cyclohexane/cyclopropane (0.9/0.1) mixture by 4.32 % and 7.47 % for 140 °C and 170 °C supply temperatures respectively. Also increasing the IHX  $\Delta T_{pp}$  from 10 K to 30 K decreased the COP of the cyclohexane/cyclopropane (0.9/0.1) mixture by 6.3 % and 6.8 % for 140 °C and 170 °C supply temperatures respectively.
- v. The aim of attaining a mixture with high critical temperature and consequently having an overall subcritical operation was met. For the best performing mixture (cyclohexane/cyclopropane), a critical temperature of 265.07 °C was attained which is far above the 204.43 °C compressor discharge temperature (CDT) of the system at 170 °C supply temperature.

The results obtained from this study represent a promising step towards the integration of the studied mixtures of cyclohexane, especially cyclohexane/cyclopropane in HTHPs. With the obtained range of supply temperatures, this integration can find its application for process heat supply in the food, cloth, chemical and metal industries. In relation to the literature presented in Table 1, the obtained results bridges the literature gap in higher supply temperature as well as novel mixtures. From a broader perspective, the realisation of the quest for the replacement of gas boilers with HTHPs for increased energy efficiency and sustainability takes a step further, with these positive results. However, this study proposes future works especially on the mixability of the studied mixtures as well as their practical application to specific industrial processes. Besides, studies on the cost implication as well as the compatibility of commercially available components of the system with the operating parameters obtained from this study, are part of future work. Resolving these issues is surely the right step towards translating these theoretical findings into practical applications.

#### CRedit authorship contribution statement

**Echezona Obika:** Writing – review & editing, Writing – original draft, Software, Formal analysis. **Florian Heberle:** Writing – review & editing, Supervision, Investigation. **Dieter Brüggemann:** Writing – review & editing, Supervision, Resources.

#### Declaration of competing interest

The authors declare that they have no known competing financial interests or personal relationships that could have appeared to influence the work reported in this paper.

#### Data availability

Data will be made available on request.

#### Acknowledgement

The authors acknowledge the German Academic Exchange Service (DAAD), Germany and the Petroleum Technology Development Fund (PTDF), Nigeria, for funding this research work. Also the Deutsche Forschungsgemeinschaft (DFG, German Research Foundation) - 491183248 and Open Access Publishing Fund of the University of Bayreuth, Germany, for funding the publication.

Cond	Condenser
COP	Coefficient of Performance
CP	Critical Pressure
CT	Critical temperature
Cycpropane	Cyclopropane
Cyhex	Cyclohexane
Exp	Expansion valve
Evap	Evaporator
IHX	Internal Heat Exchanger
GWP	Global Warming Potential
°C	Degree Celsius
HTHP	High Temperature Heat Pump
K	Kelvin
kW	Kilowatt
MM	Hexamethyldisiloxane
NBP	Normal Boiling Point
ODP	Ozone Depletion Potential
$Q_{cond}$	Heat transferred to the condenser
$W_{comp}$	Power input to the compressor
$T,s$ -diagram	Temperature Entropy Diagram
$\eta_{is}$	Compressor isentropic efficiency
$e_d$	Exergy Destruction
$m_{so}$	Heat source mass flow rate
$m_{si}$	Heat sink mass flow rate
$\dot{m}$	Mass flowrate of working fluid
$\Delta T_{pp}$	Minimum pinch temperature difference
$\dot{EX}$	Exergy flow

## References

- [1] Bengtsson P, Eikevik T. Reducing the global warming impact of a household heat pump dishwasher using hydrocarbon refrigerants. *Appl Therm Eng* 2016;99:1295–302. <https://doi.org/10.1016/j.applthermaleng.2016.02.018>.
- [2] Heinz A, Rieberer R. Energetic and economic analysis of a PV-assisted air-to-water heat pump system for renovated residential buildings with high-temperature heat emission system. *Appl Energy* 2021;293:116953. <https://doi.org/10.1016/j.apenergy.2021.116953>.
- [3] Reiners T, Gross M, Altieri L, Wagner H-J, Bertsch V. Heat pump efficiency in fifth generation ultra-low temperature district heating networks using a wastewater heat source. *Energy* 2021;236:121318. <https://doi.org/10.1016/j.energy.2021.121318>.
- [4] Arabkoohsar A, Alsagri AS. A new generation of district heating system with neighborhood-scale heat pumps and advanced pipes, a solution for future renewable-based energy systems. *Energy* 2020;193:116781. <https://doi.org/10.1016/j.energy.2019.116781>.
- [5] Nord N, Løve Nielsen EK, Kauko H, Tereshchenko T. Challenges and potentials for low-temperature district heating implementation in Norway. *Energy* 2018;151:889–902. <https://doi.org/10.1016/j.energy.2018.03.094>.
- [6] Bamigbetan O, Eikevik TM, Nekså P, Bantle M, Schlemminger C. Theoretical analysis of suitable fluids for high temperature heat pumps up to 125 °C heat delivery. *Int J Refrig* 2018;92:185–95. <https://doi.org/10.1016/j.ijrefrig.2018.05.017>.
- [7] Kosmadakis G. Estimating the potential of industrial (high-temperature) heat pumps for exploiting waste heat in EU industries. *Appl Therm Eng* 2019;156:287–98. <https://doi.org/10.1016/j.applthermaleng.2019.04.082>.
- [8] Bamigbetan O, Eikevik TM, Nekså P, Bantle M, Schlemminger C. The development of a hydrocarbon high temperature heat pump for waste heat recovery. *Energy* 2019;173:1141–53. <https://doi.org/10.1016/j.energy.2019.02.159>.
- [9] Wu Di, Yan H, Hu B, Wang RZ. Modeling and simulation on a water vapor high temperature heat pump system. *Energy* 2019;168:1063–72. <https://doi.org/10.1016/j.energy.2018.11.113>.
- [10] Wu Di, Jiang J, Hu B, Wang RZ. Experimental investigation on the performance of a very high temperature heat pump with water refrigerant. *Energy* 2020;190:116427. <https://doi.org/10.1016/j.energy.2019.116427>.
- [11] Lu Z, Gong Y, Yao Y, Luo C, Ma W. Development of a high temperature heat pump system for steam generation using medium-low temperature geothermal water. *Energy Proc* 2019;158:6046–54. <https://doi.org/10.1016/j.egypro.2019.01.513>.
- [12] Hengel F, Heschl C, Inschlag F, Klanatsky P. System efficiency of pvt collector-driven heat pumps. *Int J Thermofluids*. 2020;5–6:100034. <https://doi.org/10.1016/j.ijft.2020.100034>.
- [13] Hassan AH, Corberán JM, Ramirez M, Trebilcock-Kelly F, Payá J. A high-temperature heat pump for compressed heat energy storage applications: design, modeling, and performance. *Energy Rep* 2022;8:10833–48. <https://doi.org/10.1016/j.egypr.2022.08.201>.
- [14] Zhu T, Ommen T, Meesenburg W, Thorsen JE, Elmegaard B. Steady state behavior of a booster heat pump for hot water supply in ultra-low temperature district heating network. *Energy* 2021;237:121528. <https://doi.org/10.1016/j.energy.2021.121528>.
- [15] Al-Falahat AM, Qadourah JA, Alrwashdeh SS, khater R, Qatlama Z, Alddibs E, et al. Energy performance and economics assessments of a photovoltaic-heat pump system. *Results in Engineering* 2022;13:100324. <https://doi.org/10.1016/j.rineng.2021.100324>.
- [16] Šarevski MN, Šarevski VN. Thermal characteristics of high-temperature R718 heat pumps with turbo compressor thermal vapor recompression. *Appl Therm Eng* 2017;117:355–65. <https://doi.org/10.1016/j.applthermaleng.2017.02.035>.
- [17] Zou H, Li X, Tang M, Wu J, Tian C, Butrymowicz D, et al. Temperature stage matching and experimental investigation of high-temperature cascade heat pump with vapor injection. *Energy* 2020;212:118734. <https://doi.org/10.1016/j.energy.2020.118734>.
- [18] Wu X, Xing Z, He Z, Wang X, Chen W. Performance evaluation of a capacity-regulated high temperature heat pump for waste heat recovery in dyeing industry. *Appl Therm Eng* 2016;93:1193–201. <https://doi.org/10.1016/j.applthermaleng.2015.10.075>.
- [19] Yang W-W, Cao X-Q, He Y-L, Yan F. Theoretical study of a high-temperature heat pump system composed of a CO 2 transcritical heat pump cycle and a R152a subcritical heat pump cycle. *Appl Therm Eng* 2017;120:228–38. <https://doi.org/10.1016/j.applthermaleng.2017.03.098>.
- [20] Wu J, Sun S, Song Q, Wang D, Sun D. Subcritical recuperative air-to-water heat pump with zeotropic mixtures: comparative and performance assessment. *Energy Rep* 2022;8:13682–97. <https://doi.org/10.1016/j.egypr.2022.10.058>.
- [21] Luo B, Zou P. Performance analysis of different single stage advanced vapor compression cycles and refrigerants for high temperature heat pumps. *Int J Refrig* 2019;104:246–58. <https://doi.org/10.1016/j.ijrefrig.2019.05.024>.
- [22] Arpagaus C, Bless F, Uhlmann M, Schiffmann J, Bertsch SS. High temperature heat pumps: market overview, state of the art, research status, refrigerants, and application potentials. *Energy* 2018;152:985–1010. <https://doi.org/10.1016/j.energy.2018.03.166>.
- [23] Zühlsdorf B, Jensen JK, Cignitti S, Madsen C, Elmegaard B. Analysis of temperature glide matching of heat pumps with zeotropic working fluid mixtures for different temperature glides. *Energy* 2018;153:650–60. <https://doi.org/10.1016/j.energy.2018.04.048>.
- [24] Yelishala SC, Kannaiyan K, Sadr R, Wang Z, Levendis YA, Metghalchi H. Performance maximization by temperature glide matching in energy exchangers of cooling systems operating with natural hydrocarbon/CO2 refrigerants. *Int J Refrig* 2020;119:294–304. <https://doi.org/10.1016/j.ijrefrig.2020.08.006>.
- [25] Dai B, Liu C, Liu S, Wang D, Wang Q, Zou T, et al. Life cycle techno-economic assessment of dual-temperature evaporation transcritical CO2 high-temperature heat pump systems for industrial waste heat recovery. *Appl Therm Eng* 2023;219:119570. <https://doi.org/10.1016/j.applthermaleng.2022.119570>.
- [26] Dai B, Zhao P, Liu S, Su M, Zhong D, Qian J, et al. Assessment of heat pump with carbon dioxide/low-global warming potential working fluid mixture for drying

- process: energy and emissions saving potential. *Energy Convers Manag* 2020;222: 113225. <https://doi.org/10.1016/j.enconman.2020.113225>.
- [27] Verdnik M, Rieberer R. Influence of operating parameters on the COP of an R600 high-temperature heat pump. *Int J Refrig* 2022;140:103–11. <https://doi.org/10.1016/j.ijrefrig.2022.05.010>.
- [28] Fernández-Moreno A, Mota-Babiloni A, Giménez-Prades P, Navarro-Esbrí J. Optimal refrigerant mixture in single-stage high-temperature heat pumps based on a multiparameter evaluation. *Sustain Energy Technol Assessments* 2022;52: 101989. <https://doi.org/10.1016/j.seta.2022.101989>.
- [29] Mota-Babiloni A, Mateu-Royo C, Navarro-Esbrí J, Barragán-Cervera Á. Experimental comparison of HFO-1234ze(E) and R-515B to replace HFC-134a in heat pump water heaters and moderately high temperature heat pumps. *Appl Therm Eng* 2021;196:117256. <https://doi.org/10.1016/j.applthermaleng.2021.117256>.
- [30] Navarro-Esbrí J, Mota-Babiloni A. Experimental analysis of a high temperature heat pump prototype with low global warming potential refrigerant R-1336mzz(Z) for heating production above 155 °C. *Int. J. Thermofluids*. 2023;17:100304. <https://doi.org/10.1016/j.ijft.2023.100304>.
- [31] Dai B, Liu X, Liu S, Zhang Y, Zhong D, Feng Y, et al. Dual-pressure condensation high temperature heat pump system for waste heat recovery: energetic and exergetic assessment. *Energy Convers Manag* 2020;218:112997. <https://doi.org/10.1016/j.enconman.2020.112997>.
- [32] Heberle F, Preißinger M, Brüggemann D. Zeotropic mixtures as working fluids in Organic Rankine Cycles for low-enthalpy geothermal resources. *Renew Energy* 2012;37(1):364–70. <https://doi.org/10.1016/j.renene.2011.06.044>.
- [33] Sun S, Guo H, Gong M. Thermodynamic analysis of single-stage compression air-source heat pumps with different recuperation ways for large temperature lift. *Int J Refrig* 2019;108:91–102. <https://doi.org/10.1016/j.ijrefrig.2019.09.006>.
- [34] Deng N, Gao J, Cai R, Jing X, Zhang Y, Hao R, et al. Experimental investigation on matching a conventional water source heat pump with different refrigerants for supplying high temperature water. *Appl Therm Eng* 2020;166:114668. <https://doi.org/10.1016/j.applthermaleng.2019.114668>.
- [35] Xu C, Yang H, Yu X, Ma H, Chen M, Yang M. Performance analysis for binary mixtures based on R245fa using in high temperature heat pumps. *Energy Convers Manag* 2021;12:100123. <https://doi.org/10.1016/j.ecmx.2021.100123>.
- [36] Sun S, Guo H, Lu D, Bai Y, Gong M. Performance of a single-stage recuperative high-temperature air source heat pump. *Appl Therm Eng* 2021;193:116969. <https://doi.org/10.1016/j.applthermaleng.2021.116969>.
- [37] Gómez-Hernández J, Grimes R, Briongos JV, Marugán-Cruz C, Santana D. Carbon dioxide and acetone mixtures as refrigerants for industry heat pumps to supply temperature in the range 150–220 °C. *Energy* 2023;269:126821. <https://doi.org/10.1016/j.energy.2023.126821>.
- [38] Navarro-Esbrí J, Fernández-Moreno A, Mota-Babiloni A. Modelling and evaluation of a high-temperature heat pump two-stage cascade with refrigerant mixtures as a fossil fuel boiler alternative for industry decarbonization. *Energy* 2022;254: 124308. <https://doi.org/10.1016/j.energy.2022.124308>.
- [39] Zhang Y, Zhang Y, Yu X, Guo J, Deng N, Dong S, et al. Analysis of a high temperature heat pump using BY-5 as refrigerant. *Appl Therm Eng* 2017;127: 1461–8. <https://doi.org/10.1016/j.applthermaleng.2017.08.072>.
- [40] Yan H, Ding L, Sheng B, Dong X, Zhao Y, Zhong Q, et al. Performance prediction of HFC, HC, HFO and HCFO working fluids for high temperature water source heat pumps. *Appl Therm Eng* 2021;185:116324. <https://doi.org/10.1016/j.applthermaleng.2020.116324>.
- [41] Pan L, Wang H, Chen Q, Chen C. Theoretical and experimental study on several refrigerants of moderately high temperature heat pump. *Appl Therm Eng* 2011;31 (11–12):1886. <https://doi.org/10.1016/j.applthermaleng.2011.02.035>. –93.
- [42] Kristensen AS, Sørensen EK, Madsen C, Kristófersson J, Forooghi P. Performance analysis of heat pumps with zeotropic mixtures at different load conditions. *Int J Refrig* 2023;145:264–75. <https://doi.org/10.1016/j.ijrefrig.2022.09.028>.
- [43] Zhang X, Wang F, Liu Z, Gu J, Zhu F, Yuan Q. Performance research on heat pump using blends of R744 with eco-friendly working fluid. *Procedia Eng* 2017;205: 2297–302. <https://doi.org/10.1016/j.proeng.2017.10.094>.
- [44] Jiang J, Hu B, Wang RZ, Deng N, Cao F, Wang C-C. A review and perspective on industry high-temperature heat pumps. *Renew Sustain Energy Rev* 2022;161: 112106. <https://doi.org/10.1016/j.rser.2022.112106>.
- [45] Querol E, Gonzalez-Regueral B, Ramos A, Perez-Benedito JL. Novel application for exergy and thermoeconomic analysis of processes simulated with Aspen Plus®. *Energy* 2011;36(2):964–74. <https://doi.org/10.1016/j.energy.2010.12.013>.
- [46] Haydary J. *Chemical process design and simulation: Aspen Plus and Aspen HYSYS applications*. Hoboken, NJ: John Wiley & Sons, Inc; American Institute of Chemical Engineers; 2019.
- [47] Huber ML, Lemmon EW, Bell IH, McLinden MO. The NIST REFPROP database for highly accurate properties of industrially important fluids. *Ind Eng Chem Res* 2022; 61(42):15449–72. <https://doi.org/10.1021/acs.iecr.2c01427>.
- [48] Marina A, Spoelstra S, Zondag HA, Wemmers AK. An estimation of the European industrial heat pump market potential. *Renew Sustain Energy Rev* 2021;139: 110545. <https://doi.org/10.1016/j.rser.2020.110545>.
- [49] Jiang J, Hu B, Wang RZ, Deng N, Cao F, Wang C-C. A review and perspective on industry high-temperature heat pumps. *Renew Sustain Energy Rev* 2022;161: 112106. <https://doi.org/10.1016/j.rser.2022.112106>.
- [50] Jodeiri AM, Goldsworthy MJ, Buffa S, Cozzini M. Role of sustainable heat sources in transition towards fourth generation district heating – a review. *Renew Sustain Energy Rev* 2022;158:112156. <https://doi.org/10.1016/j.rser.2022.112156>.
- [51] Ozgener L, Hepbasli A, Dincer I. A key review on performance improvement aspects of geothermal district heating systems and applications. *Renew Sustain Energy Rev* 2007;11(8):1675–97. <https://doi.org/10.1016/j.rser.2006.03.006>.
- [52] Ziemele J, Kalnins R, Vīgants G, Veidenbergs I. Evaluation of the industrial waste heat potential for its recovery and integration into a fourth generation district heating system. *Energy Proc* 2018;147:315–21. <https://doi.org/10.1016/j.egypro.2018.07.098>.
- [53] Bahrami M, Pourfayaz F, Kasaiean A. Low global warming potential (GWP) working fluids (WFs) for Organic Rankine Cycle (ORC) applications. *Energy Rep* 2022;8:2976–88. <https://doi.org/10.1016/j.egypr.2022.01.222>.
- [54] ONU Environnement. *Montreal Protocol on substances that deplete the ozone layer. In: 2022 report of the refrigeration, air conditioning and heat pumps technical options committee (RTOC). 2022 assessment*. UNEP (United Nations Environment Programme); 2023.
- [55] Drescher U, Brüggemann D. Fluid selection for the Organic Rankine Cycle (ORC) in biomass power and heat plants. *Appl Therm Eng* 2007;27(1):223–8. <https://doi.org/10.1016/j.applthermaleng.2006.04.024>.
- [56] Lai NA, Wendland M, Fischer J. Working fluids for high-temperature organic Rankine cycles. *Energy* 2011;36(1):199–211. <https://doi.org/10.1016/j.energy.2010.10.051>.
- [57] Saleh B, Koglbauer G, Wendland M, Fischer J. Working fluids for low-temperature organic Rankine cycles. *Energy* 2007;32(7):1210–21. <https://doi.org/10.1016/j.energy.2006.07.001>.
- [58] Yang J, Li J, Yang Z, Duan Y. Thermodynamic analysis and optimization of a solar organic Rankine cycle operating with stable output. *Energy Convers Manag* 2019; 187:459–71. <https://doi.org/10.1016/j.enconman.2019.03.021>.
- [59] Yan YL, Zhang SY, Ge Z, Xie ZY, Huang GD, Yuan ZP. Performance analysis of solar organic rankine cycle with stable output using cyclopentane/cyclohexane mixtures. *Fuel Cell* 2021;21(1):66–76. <https://doi.org/10.1002/fuce.202000053>.
- [60] Oyekale J, Heberle F, Petrollese M, Brüggemann D, Cau G. Thermo-economic evaluation of actively selected siloxane mixtures in a hybrid solar-biomass organic Rankine cycle power plant. *Appl Therm Eng* 2020;165:114607. <https://doi.org/10.1016/j.applthermaleng.2019.114607>.
- [61] Chen Z, Wang Y, Zhang X. Energy and exergy analyses of S-CO<sub>2</sub> coal-fired power plant with reheating processes. *Energy* 2020;211:118651. <https://doi.org/10.1016/j.energy.2020.118651>.
- [62] Jain V, Sachdeva G, Kachhwaha SS, Patel B. Thermo-economic and environmental analyses based multi-objective optimization of vapor compression-absorption cascaded refrigeration system using NSGA-II technique. *Energy Convers Manag* 2016;113:230–42. <https://doi.org/10.1016/j.enconman.2016.01.056>.
- [63] Linteris GT, Bell IH, McLinden MO. An empirical model for refrigerant flammability based on molecular structure and thermodynamics. *Int J Refrig* 2019; 104:144–50. <https://doi.org/10.1016/j.ijrefrig.2019.05.006>.